Available online at www.sciencedirect.com

SCIENCE DIRECT®

Journal of Volcanology and Geothermal Research 137 (2004) 169–185

Journal of volcanology and geothermal research

www.elsevier.com/locate/jvolgeores

Vent discrimination at Stromboli Volcano, Italy

April D. McGreger, Jonathan M. Lees*

Department of Geological Sciences, University of North Carolina, Chapel Hill, USA

Abstract

Eruptive activity at Stromboli Volcano was significantly elevated over background levels in May 2001. During 63 h of observation, eight vents produced, on average, 17 explosions/h with an average repose interval of 3 min. During this period, the Stromboli vents exhibited consistent seismic and acoustic signatures, based on cross-correlation cluster analysis. Dendrogram clustering, based on waveform cross-correlation, was used to illustrate the complexity of the near surface plumbing system of Stromboli's multi-vent edifice. Cross-correlations of displacement seismograms produced by explosions at specific craters, such as the Northeast crater (NEC), form dense waveform clusters with correlation coefficients between 0.96 and 0.99, while displacement waveforms from other craters, such as the Southwest crater (SWC), exhibit loose clusters with correlations between 0.88 and 0.96. The inconsistency of SWC events, as compared to the NEC, suggests that the vent system there is more heterogeneous. Cluster linkage distance between the NEC cluster and the Central crater (CC) cluster is shorter than the linkage distance between the NEC and SWC clusters, indicating that NEC and CC are more closely related. Infrasonic observations were used to locate vent explosions confirming that the clusters of events are associated with specific vents or craters. Qualitative analyses of acoustic waveforms from approximately 500 explosions reveal that impulsive acoustic signals were associated with short, mechanically simple ground displacement responses. These events may correspond to the bursting of an individual gas slug. Similar degassing mechanisms from vents in the NEC and the CC show common characteristics in their displacement waveforms.

Keywords: cluster analysis; Stromboli; volcano seismology; acoustics

1. Introduction

Stromboli Volcano is a 12.6-km^2 composite cone that rises 3500 m above the seafloor to an elevation of 924 m. In May 2001, the summit region contained three active craters with eight active vents (Fig. 1). Stromboli's relatively mild explosive nature makes it a convenient natural laboratory for the study of a variety of volcanic phenomena because geophysical monitors may be deployed within a few hundreds of meters of the explosion source. Regular "Strombolian" explosions, observed in historic times, consist of ejections of ash, lapilli, lava bombs, and vapor emission at a rate of 3–10 explosions per hour with volumetric rates of 10^4 m^3 s^{-1} (Chouet et al., 1974). Although mild Strombolian activity represents the dominant feature of the volcano, Stromboli Volcano exhibits a variety of behaviors, including occasional swarm activity with as many as 20–30 events per hour (Chouet et al., 1999), a few weeks per year of quiescence (Ripepe et al., 1996), periods of vigorous activity and occasional lava

* Corresponding author. Fax: +1-919-966-4519.
E-mail addresses: mcgreger@email.unc.edu (A.D. McGreger), jonathan_lees@unc.edu (J.M. Lees).

0377-0273/$ - see front matter © 2004 Published by Elsevier B.V.
doi:10.1016/j.jvolgeores.2004.05.007

flows, the most recent of which occurred in December 2002 (personal communication, Marco Fuller, http://www.strombolionline.com/). Ballistics may reach heights ranging from a few meters to a few hundred meters, with muzzle velocities ranging between 50 and 100 m s^{-1} (Chouet et al., 1974).

Explosions at Stromboli are generated by the bursting of an over pressurized bubble at the surface of the magma column (Blackburn et al., 1976; Wilson et al., 1980). The bubbles form intermittently in the top few hundred of meters of the cone by the coalescence of a foam layer in a shallow magma chamber (Jaupart and Vergniolle, 1988, 1989; Vergniolle and Jaupart, 1990). This coalescence may occur spontaneously or may be forced beneath a structural barrier (Ripepe and Gordeev, 1999). Persistent Strombolian activity has been documented for over 2000 years suggesting an efficient gas–magma transport system. The location of the crater terrace has shown great stability as well, with no significant change in the last 400 years (Washington, 1917).

2. Previous work

Many experiments have been conducted in recent years to gain a better understanding of Stromboli's seismic and acoustic wavefields. The implementation of infrasonic monitoring at Stromboli (Braun and Ripepe, 1993; Buckingham and Garces, 1996; Ripepe, 1996; Ripepe and Gordeev, 1999) has proved an invaluable tool for understanding how seismic signals are produced by volcanic activity. Infrasonic monitoring reveals that the high-frequency portion of some seismic signals can be attributed to ground-coupled airwaves produced during an explosion (Braun and Ripepe, 1993). Volcanic tremor at Stromboli has also been correlated to rhythmical infrasonic transients that are thought to be associated with small ($\sim$ 0.5 m) gas bubble bursts (Ripepe and Gordeev, 1999; Ripepe et al., 1996). Synchronized analysis of seismic and acoustic signals with video recordings has provided a platform for the investigation of volcano explosion dynamics at Stromboli (Chouet et al., 1974; Blackburn et al., 1976; Ripepe et al., 1993; Vergniolle and Brandeis, 1994). Shallow conduit vibrations and associated explosions have been modeled on several volcanoes as resonant waves, where frequency domain representations of seismo-acoustic wavefields are simulated and used to estimate conduit parameters (Garces, 1997, 2000; Garces and McNutt, 1997). Resonance, as seen at Arenal Volcano, Costa Rica (Garces et al., 1998), and Karymsky Volcano, Russia (Johnson et al., 1998), is generally not observed at Stromboli, however. Strombolian volcanic explosions have been previously modeled by the expansion and rupture of gas bubbles at the surface of the Northeast vents (Vergniolle et al., 1996). The long-period ($\sim$10 s) seismic signals observed at Stromboli in 1997 were modeled successfully for source moment inversion (Chouet et al., 2003). In the present paper, we examine both the acoustic and the seismic wavefields showing the reproducibility of signals related to deformation at individual conduits associated with specific vent explosions. Our paper is aimed at the discrimination of vents and explosions where numerous vents are active simultaneously and few seismic stations are available for analysis. We show that with a small number of stations (less than three), it is possible to discriminate conduit activity in the subsurface plumbing system.

Broadband seismic records at Stromboli commonly exhibit very low-frequency (VLP) signals, often with periods of 10 s or more (Chouet et al., 1999; Neuberg et al., 1994). The source-time functions of these signals are characterized by a compression–dilation–compression motion (Chouet et al., 1999). Moment tensor inversion of long-period signals from two different vents at Stromboli, using data recorded in 1997, indicated source centroids at 220 and 260 m beneath the summit, and located approximately 160 m northwest of the active vents. The inversion models invoked cracks dipping at about 60° where a piston effect of a gas slug deforms the surrounding rocks in the conduit (Chouet et al., 2003).

Shortly after volcanic explosions were first recorded seismically at Stromboli, various methods were used to classify the waveforms into groups (Lo Bascio et al., 1973; Del Pezzo et al., 1975; Schick, 1981). Other authors have since contributed to the organization of Strombolian events into classes (Ntepe and Dorel, 1990; Falsaperla and Schick, 1993; Ripepe et al., 1993). The repetitive action of explosion sources at Stromboli has been documented by numerous researchers (Beinat et al., 1994; Chouet et al., 1999; Falsaperla et al., 1998; Neuberg and Luckett,

1996; Ntepe and Dorel, 1990) and waveform classifications have been linked to specific craters or source locations (Neuberg and Luckett, 1996; Chouet et al., 1999, 2003). It has further been suggested that these waveform classes are not directly linked to crater geometry but depend instead on gas pressure fluctuations (Ripepe et al., 1993).

In this paper, seismic and acoustic waveforms from over 500 events are used to establish a quantitative classification of vent explosions using cross-correlation cluster analysis. We present results which show that each vent contributes a characteristic seismic waveform that enables us to distinguish vent activity in the absence of visual observations. Acoustic travel time differentials are further used to help pinpoint specific vents that co-exist within tens of meters of each other. Because visibility is often degraded on active volcanoes, we emphasize the importance of being able to isolate specific vent activity during eruptive episodes. Furthermore, the identification of the precise sequence of events during eruptions provides a valuable indicator for hazard mitigation and assessment. Finally, detailed identification of vent activity is necessary for establishing a description of conduit geometry in the shallow structure of the volcano. We show that in 2001 activity included more varied signals than those determined in 1997, and was distributed among the eight active vents.

3. Summit activity

Explosive activity at Stromboli in May 2001 was especially intense. During the 63 h of observation

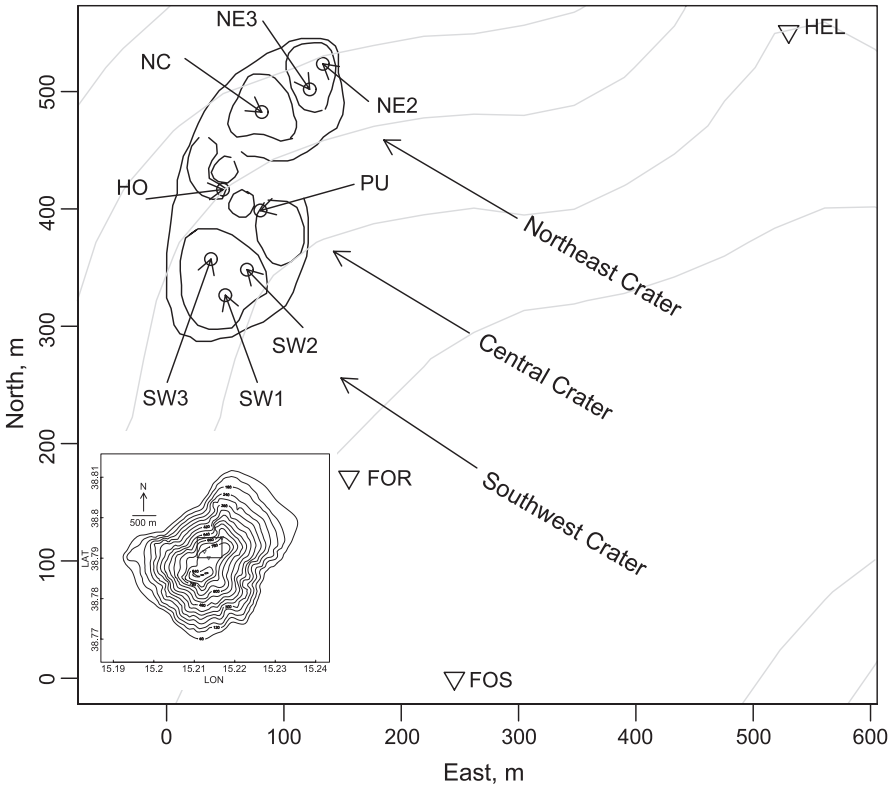

Fig. 1. Map of Stromboli with station configuration. Stations, marked by triangles (FOR, FOS, and HEL) include three-component, broadband sensors equipped with infrasonic microphones. The summit area is divided into three craters: Southwest (SWC), Central Crater (CC) and Northeast (NEC), with eight active vents marked by circles (SW1, SW2, SW3; PU, HO; NC, NE2, NE3). Vents in the SWC and NEC were determined by ejecta trajectory. Inset shows Stromboli island with the detailed map boxed for reference. Line drawing adapted from Andy Harris, 2001.

reported in this paper, eight summit vents were active, producing an average of 17 explosions per hour. The recorded activity differs considerably from large, single-vent Strombolian volcanoes like Arenal Volcano, Costa Rica (Benoit and McNutt, 1997), Karymsky Volcano, Kamchatka or Sangay Volcano, Ecuador, (Johnson and Lees, 2000) where most explosions share consistent characteristics over days or even years. Karymsky, for example, exhibited Strombolian style activity over a period of 3 years (1996–1999) often including as many as 15 explosions per hour, although the explosions appear to have come from

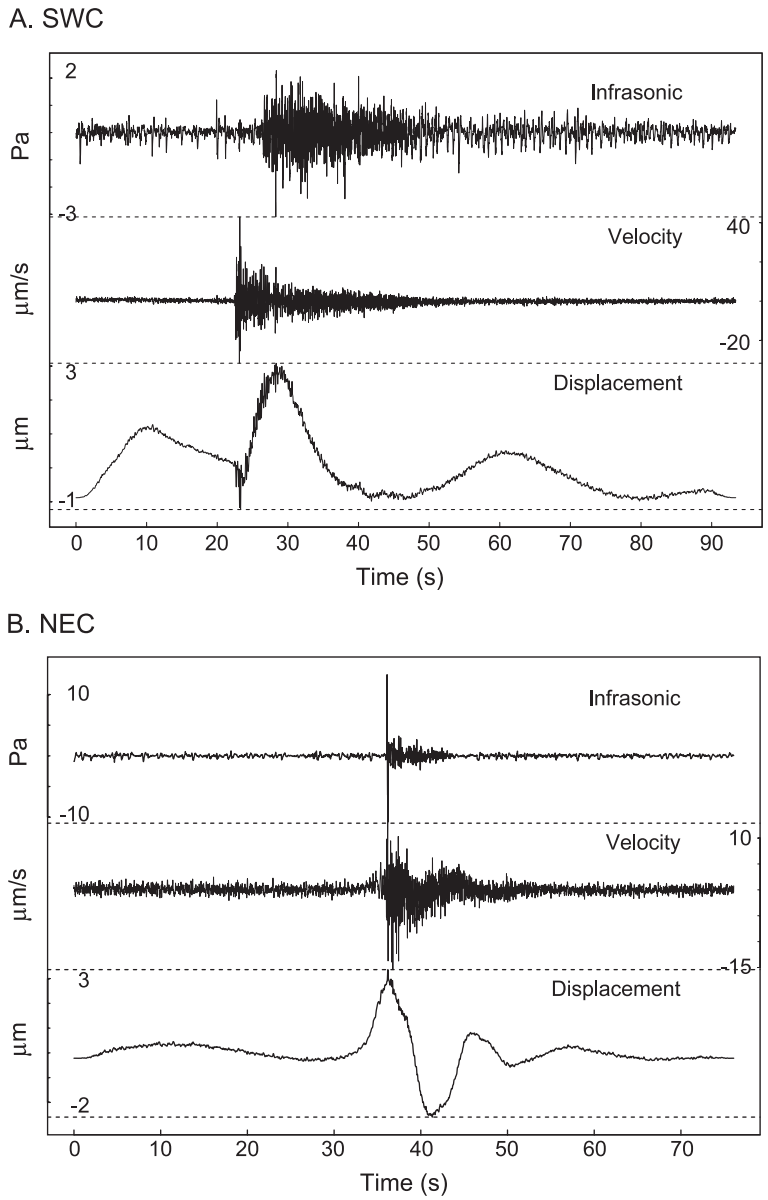

Fig. 2. Example waveforms for five classes of eruptions. Infrasound, vertical velocity seismograms, and corresponding vertical displacement seismograms are shown for characteristic events of each cluster (A) SWC; (B) NEC (vents NE2 or NE3); (C) NC (of the NEC); (D) HO and (E) PU. All events shown recorded at station FOR.

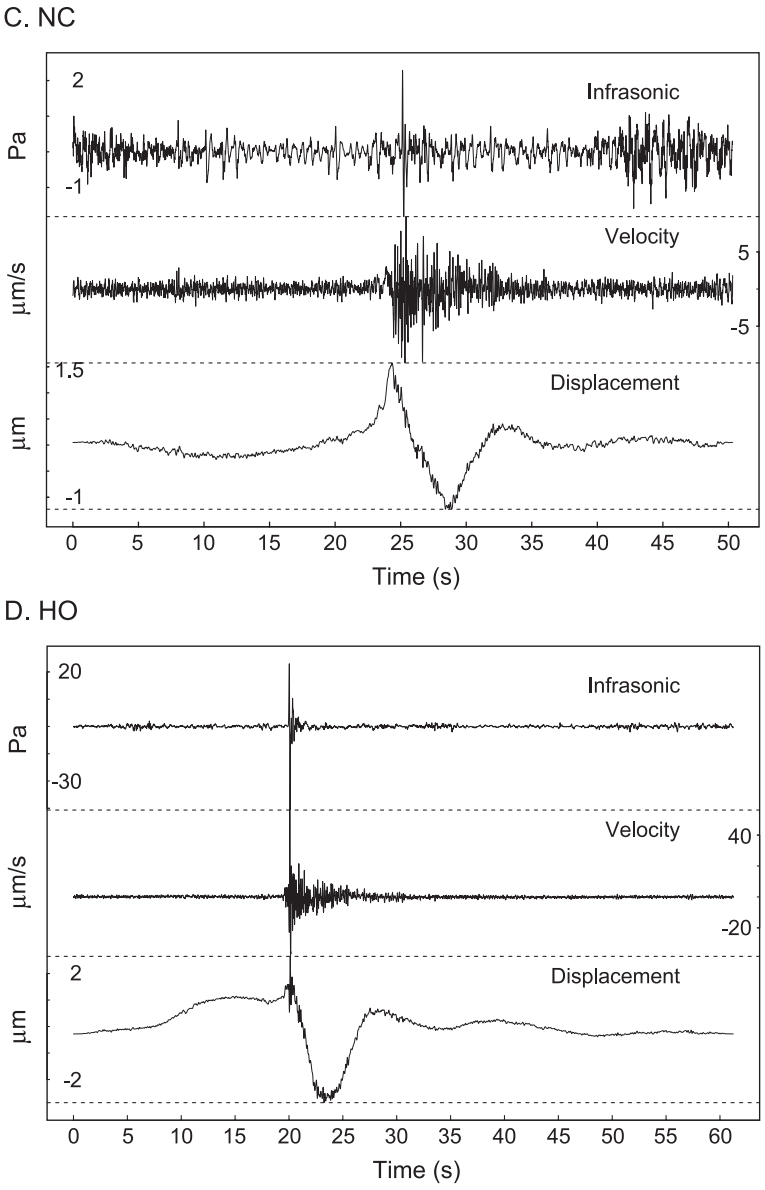

Fig. 2 (*continued*).

one vent and are repetitive in waveform signature during recording sessions that lasted several days. At Stromboli, in 2001, on the other hand, each of the eight active vents appeared to produce specific signals with characteristics which were clearly distinguishable, even through simple visual and audio observation. The fact that these vents, located within tens or hundreds of meters of each other, consistently exhibit a unique and distinguishable character, suggests that the vents have a non-destructive source situated in the shallow plumbing system of the volcano edifice.

The summit of Stromboli is composed of three main craters positioned along a rough line running Northeast to Southwest (Fig. 1). During the month of May, 2001, three vents were active in the Southwest crater (SWC), which produced sustained (20–40 s),

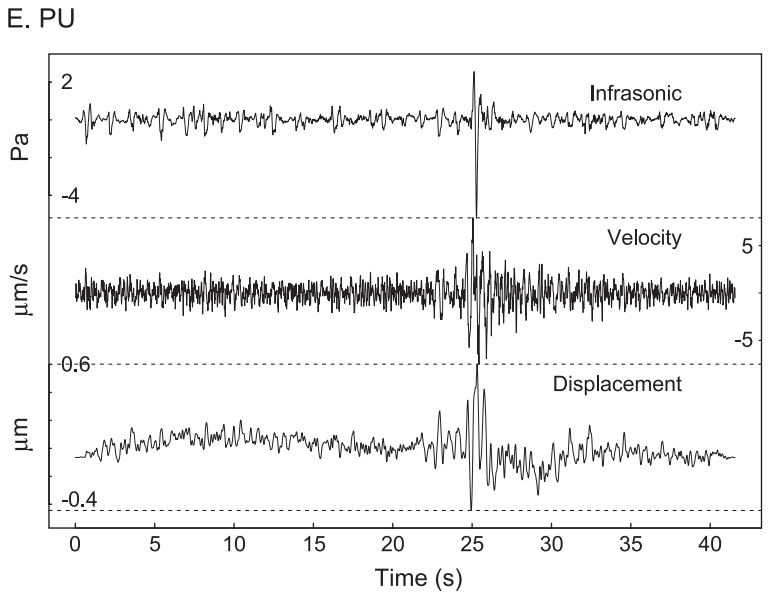

Fig. 2 (*continued*).

dark ash columns reaching up to 350 m including minor to heavy incandescent fans of ejecta (personal communication, Andy Harris, 2001). Explosions in the SWC occurred intermittently, approximately twice per hour (Fig. 2A).

Three vents in the Northeast Crater (NEC) consisted of well collimated, gas-rich eruptions containing little to no ash with minor bombs reaching heights of 200–300 m. Eruptions averaged 10 to 20 s in duration based upon visual observations. From time differences of acoustic arrival times at two microphone sites (Table 1), eruptions from the westernmost vent (NC, Figs. 1 and 2C) were distinguishable from the two easternmost vents (NE2 and NE3). A strong, VLP signal (~ 10 s) was present in events associated with the NEC, notably associated with vents NE2 and NE3 (Fig. 2B).

During the 2001 broadband deployment, two active vents were observed in the Central Crater (CC), indicated by PU and HO (Fig. 1). The "puffer" (PU) vent received its name from the puffs of gas that were released at approximately 1-s intervals (Fig. 2E). This passive degassing is unrelated to discrete Strombolian explosions and similar background infrasonic activity has been observed at Mt. Etna (Ripepe et al., 2001). Although the source of the pulses was not identified, Ripepe and Gordeev (1999) suggested that infrasonic transients generated by puffing were correlated with volcanic tremor at Stromboli. In addition to the PU vent, infrequent explosions (~ 0.4/h, personal communication, Andy Harris, 2001) were observed coming from the Hornito (HO, Figs. 1 and 2D). Explosions from the HO produced loud jet-like acoustic signals with very little associated ejecta.

4. Data

A three station broadband seismo-acoustic array was deployed around the summit craters of Stromboli Volcano, Italy (Fig. 1). Broadband instruments were co-located with infrasonic microphones to measure the seismic and acoustic wavefields produced by explosions over a period of 10 days. The stations (marked by triangles in Fig. 1) FOR and HEL were each equipped with 30-s period Guralp CMG 40T broadband seismometers and McChesney-4 element infrasonic microphones (3 dB down at ~ 2 Hz) (Johnson et al., 2003). Station FOS was equipped with a Guralp CMG 3T broadband seismometer with a 120-s period and a Larson-Davis infrasonic microphone (3 dB down at ~ 0.25 Hz). Data used in this study include signals recorded from 16:00 GMT on

May 19 through 11:00 GMT May 21, when all stations were operating, except for the damaged, vertical component of station FOS. All stations recorded seismic and acoustic data streams continuously at 125 samples s^{-1}.

From the continuous seismo-acoustic records, over 500 events were selected based on high signal-to-noise ratio and apparent lack of interference from other explosive events. Repetitive waveform classes were observed on both the acoustic and the seismic data across stations, suggesting source similarities. Of the three stations, station FOR, located near the SWC, exhibited the best signal-noise ratio and was thus used for more detailed correlation cluster analysis.

Rough topography and volcanic hazard prevented the deployment of seismic and acoustic sensors on the northwest side of the volcano. Three broadband stations were deployed: FOR and FOS were 187 and 380 m southeast of the SWC, respectively, and station HEL was 530 m northeast of the SWC (Fig. 1; Table 1). This resulted in an array that was skewed to the south relative to the active vents, and thus diminished our ability to make precise triangulation estimates of infrasonic sources. As an alternative, the time difference between first arrivals at FOR and HEL was used to distinguish sources from different craters. Table 1 provides the distances and times between vents and stations during the deployment. Assuming a homogeneous sound speed (340 m s^{-1}), we were able to discriminate infrasound sources from four primary source regions including: (1) events from the SWC; (2) events from the CC; (3) events from the NE2; and NE3 vents, and (4) events from the NC vent. Individual vent discrimination was achieved only in the NEC, where the NC vent was more than 45 m from both NE2 and NE3 (Fig. 1). Successful crater discrimination was achieved in approximately 80% of events, where a clear first arrival was detected at both stations FOR and HEL. Based on simple waveform characteristics (amplitude, frequency content, waveform shape, etc.), we were able to further differentiate events originating from the central crater into explosion-related events from the HO vent versus puffing events at the PU vent. The waveforms shown in Fig. 2 are representative of events from different classes. Characteristic acoustic and seismic waveform classes are described in the following sections.

Table 1
Relative acoustic travel time arrivals

Acoustic time differentials and source–receiver distances				
Velocity of air wave = 340 m s^{-1}				
	Delta t (s), (FOR-HEL)	Distance (m), from FOR	Distance (m), from HEL	Distance (m), from FOS
SWC				
SW1 (western)	1.05	187	529	381
SW3 (northern)	0.95	220	529	414
SW2 (eastern)	0.92	197	504	391
CC				
PU (puffer)	0.70	238	476	431
HO (hornito)	0.66	252	487	445
NEC				
NC (western)	0.36	319	454	510
NE3 (southern)	0.23	331	411	517
NE2 (eastern)	0.20	354	399	538

Travel time differences for acoustic signals at FOR and HEL are used to discriminate five sources of events: SWC; CC; NEC; and NC and PU (Fig. 1).

5. Qualitative waveform analysis

Hundreds of events recorded over the time span of the 2001 deployment were isolated, examined visually and initially classified by associated travel time differentials and general waveform shapes. For example, over a period of 18 h on May 20, 56 NEC, 32 SWC, 32 CC–NC and 47 indeterminate events were identified and catalogued for qualitative waveform cluster analysis. Once a general understanding of the broad characteristics of the signals was obtained, an automated quantitative methodology was applied to discriminate between vent explosions at the three craters and how these relate to their associated low-frequency seismic source. The following is a brief description of

general waveform morphological patterns observed in each of the major groups.

5.1. SWC

The velocity seismograms from the SWC (Fig. 2A) are dominated by high frequencies. The corresponding ground motion displacement reveals a period of 20 s and an average duration of ~60 s. The infrasonic signals from all SWC vent explosions are emergent and appear to continue for the duration of the explosion or for a few seconds post-eruption (as determined by the duration of the velocity seismogram). At times, the SWC infrasonic events are absent, or at least indistinguishable above background (wind) noise. The emergent characteristics of the infrasonic signals make it difficult to obtain clear arrival times, thus affecting time differentials and vent locations. Seismograms from the SWC explosions exhibit a 'W'-shaped displacement similar to that observed by Neuberg and Luckett (1996). The first leg of the displacement or the first "hump" of the W is towards the source in the vertical and radial component and precedes the first arrival of the velocity seismogram by about 13 ± 1 s. The seismic displacement begins as a gradual motion towards the source, followed by a stronger, more impulsive movement away from the source, which appears to coincide with the onset and duration of the velocity seismogram. The final ground motion is gradual and away from the source, lasting 20 s or more after the surface manifestation of the explosion has terminated.

5.2. NE2 and NE3

Fig. 2B shows the infrasonic, seismic velocity, and seismic displacement waveforms for a typical NEC explosion. Displacement seismograms show the onset of a long-period signal (~1 s) before the onset of the high-frequency, ground-coupled, infrasonic airwaves produced by the explosions (Braun and Ripepe, 1993). Events from the NEC produce a strong impulsive compressional signal (average about 10 ± 4 Pa at 330 m) with a typical frequency of 5 Hz, followed by a lower-amplitude, higher-frequency coda, which continues for an average of 10 s. The displacement seismogram displays initial motion away from the source followed by a strong movement towards the source that produces the characteristic "U" shape of the NEC seismic displacements. A low-frequency (3 Hz) signal starts about 3.9 s before the onset of the acoustic signal at station FOR, as measured on records rotated to radial-transverse motion.

5.3. NC

Events from the NC vent (Fig. 2D) differ slightly from events originating at the NE2 or NE3 vents. As with events from other NEC vents, displacement seismograms show the onset of a long-period signal around 1 s before the onset of the ground-coupled infrasonic wave. The infrasonic signal is generally a single oscillatory pulse, while the displacement seismogram appears V-shaped rather than U-shaped like those of NE2 and NE3 events. Displacement seismograms from the NC explosions share similar VLP signals (~10 s) and durations (~20 s) with the NE2 and NE3 events.

5.4. HO

The velocity seismogram from the HO vent (Fig. 2D) includes a low-amplitude high-frequency (23.7 ± 2.5 Hz) signal preceding the onset of the ground-coupled airwave by 0.3 to 1.0 s. Eruptions from the HO vent exhibit high peak-to-peak infrasonic amplitudes, ranging between 40 and 50 Pa at 250 m, considerably higher than explosions from the other vents. Field observations during the deployment corroborate that a substantial amount of power is present at audible frequencies. Displacement seismograms from HO share characteristics common to both the SWC and NEC displacements, where motion is dominated by a strong movement toward the source. Furthermore, HO seismic response is comparable in both duration (10–15 s) and shape to the NEC's displacement. However, the strong "U" motion is often preceded by a gradual movement away from the craters (0.62 μm) followed by a slight motion towards the source prior to the arrival of the acoustic wave. The sharp displacement away from the source is similar to displacement waveforms produced by the SWC. This gives events from the HO a lopsided W-shaped displacement with an understated first hump,

compared to SWC events, and a shorter duration (30 s compared to 60 s).

5.5. PU

Only the more powerful puffs (>3 Pa) from PU (Fig. 2E) produced signals that were consistently distinguishable above background tremor on velocity seismograms. Background acoustic noise similar to this, including constant low amplitude signals recorded every 1–2 s, has been reported previously at Mt. Etna (Ripepe et al., 2001). During the 2001 Stromboli deployment, the PU vent produced simple acoustic waveforms resembling inverted *sinc* functions ($\sin(x)/x$), repeated in a quasi-periodic manner at ~1-s intervals with a typical frequency of 2 Hz. These pulses were of relatively low amplitude (~1 Pa at 238 m), but were consistently distinguishable above background wind noise. The puffer events were not related to distinct explosions and did not generally produce a notable displacement.

6. Quantitative discrimination by cross-correlation cluster analysis

Because acoustic signals contain high frequencies and do not suffer severe contamination from path effects, common on seismic data, it is possible to triangulate these signals to determine the location of specific explosions. This was done where the data allowed clear determination of arrivals, and explosions were catalogued according the crater source. For the cluster analysis presented below, events were categorized by travel time differential (Fig. 3 and Table 1) and by qualitative patterns described above. Each event was assigned a tag, based on these associations, although the cluster analysis is derived independent of the travel-time determined event associations. It should be noted that the travel times are estimated on data that has a frequency band of 1–10 Hz, whereas cluster analysis on seismic data is determined from seismic signals filtered from 50–2-s periods. Because these frequency bands represent significantly different parts of the wavefield created by Strombolian explosions, it is remarkable that they are so closely associated.

Quantitative cluster analysis was performed on a relatively small number of events (fewer than 40 events for each set) to allow for simple display of the results in the dendrogram figures (Figs. 4 and 5). Only data collected during low wind conditions was used, because excess noise often obscures acoustic signals. Arrival time picks were made based on the following criteria: Individual signals were chosen uniformly by selecting windows that spanned the arrival of the acoustic waves by 25 s on either side, to ensure that the full displacement signal would be captured, while rejecting windows that were clearly contaminated by two or more events. PU events were not chosen because they did not correspond to explosions in the way that NEC, SWC and CC events did. Events were only selected if all channels of station FOR and the microphone at HEL were operating. For events meeting the above criteria, displacements from the vertical, north/south, and east/west seismic components were cross-correlated. Before cross-correlation, velocity seismograms were deconvolved to remove instrument response, then integrated and bandpassed with a 2–50 s, 8-order Butterworth filter, in accordance with filters used to isolate long-period, conduit events (Chouet et al., 1999, 2003). In this frequency band, the acoustic signals do not exhibit any signal, so they are excluded from the analysis. Cluster analysis was performed on the population subsets for each day of the survey individually. Subsets from May 19 to 21 were combined to evaluate the behavior of cross-correlation clusters over time. For consistency, we present here results using only seismic data from station FOR, the most reliable station during the deployment. All pairs of events on the three seismic channels recorded at station FOR were cross-correlated, i.e. vertical displacements with vertical displacements, etc. The median cross-correlation value for each event pair was used to avoid the results being skewed by noise on one channel.

The matrix of all cross-correlation scores (σ) provides a data base from which one can cluster events that are similar to each other but differ from other events in the data set. In this study, average link cluster analysis was used primarily, although alternative choices were investigated to show that clustering did not depend on the specific methodology employed. Standard cluster analysis (Hartigan, 1975; Frohlich and Davis, 1990; Lees, 1997) and tree

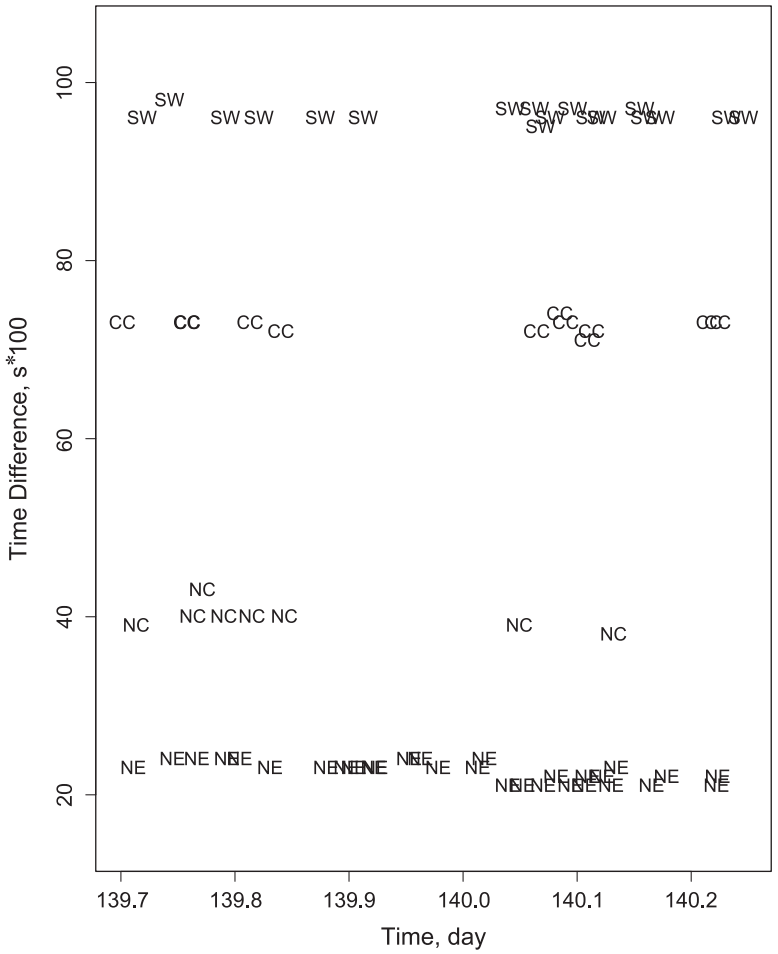

Fig. 3. Travel time differentials as a function of time for days 139–140. Plotted symbols represent craters/vents associated with individual explosions based on travel time differentials and waveform character.

diagrams (Figs. 4 and 5) were created using the software package called **R** (Ihaka and Gentleman, 1996), although our general results do not depend on a particular algorithm or software platform. Several cluster analysis programs were tested on the Stromboli waveforms, including equivalence class methods (Aster and Scott, 1993; Lees, 1998) and robust, fuzzy logic methods (Kaufman and Rousseeuw, 1990). While dendrogram results differ in details depending on the choices of methods, the broad associations illustrated in this paper are robust with respect to technique. Clusters in the examples presented below (Figs. 4 and 5) were derived using the cross-correlation pairs of events, to determine a distance matrix for the data set. (The distance is defined as the compliment of the cross-correlation score, i.e. $1-\sigma$.) Dendrogram trees were produced by partitioning events into groups, where the distance between members is measured by the average distance of the group to the other groups. Partitioning commences by associating pairs with high correlation, after which clusters are constructed by adding groups together consecutively, until the final step, when all individuals are grouped together. The dendrogram tree represents a summary of the relative association scores of each cluster in the data set.

The cluster analysis approach allows us to form groups of signals based on waveform alone, in this

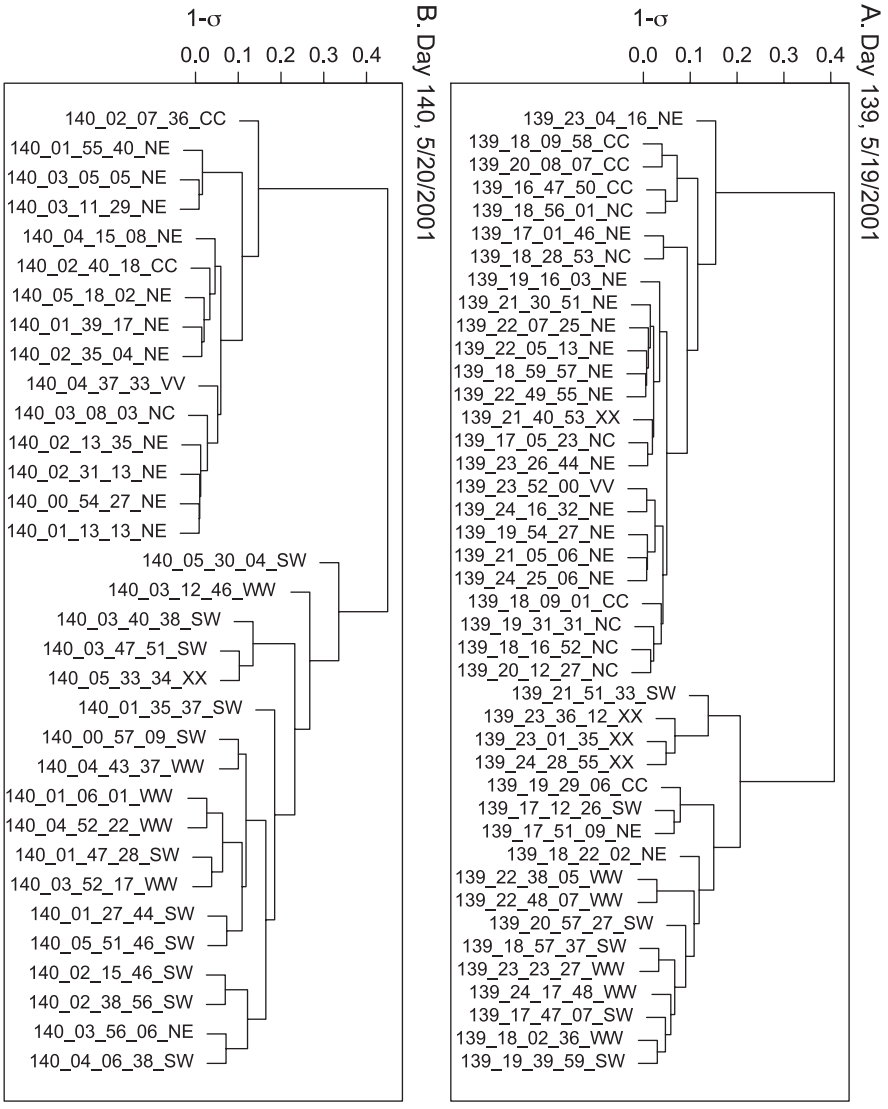

Fig. 4. Dendrograms of cluster analysis on (A) May 19 (Day 139) and (B) May 20 (Day 140). Vertical axis is the distance from one waveform cluster to another as measured by the compliment of the cross-correlation ($1-\sigma$, where σ is the maximum of the cross-correlation). Each stem is labeled with the event ID (Julian-day.hour.minute.second) and the crater or vent label associated with that travel time differential (Table 1 and Fig. 1). Events whose travel time differentials could not be determined were assigned labels X, V or W, depending on the characteristic shape of the vertical displacement seismogram. X indicates indeterminate shape.

case, from a small number of stations, or even a single recording station. During the deployment in 2001, the highly repetitive, low-frequency seismic signals, originating consistently from specific vents, requires that the geometry of the volcano be stable. While one could use visual observation or acoustic travel times to determine which vent exploded, conditions permitting, this information provides no insight into the source of the deeper, long-period signals that accompany explosions at Stromboli (Chouet et al., 1999). The low-frequency content (5–10-s periods) of the seismic signals, and the temporal consistency associated with a particular crater, suggests that conduits are distinct at a deeper level within the

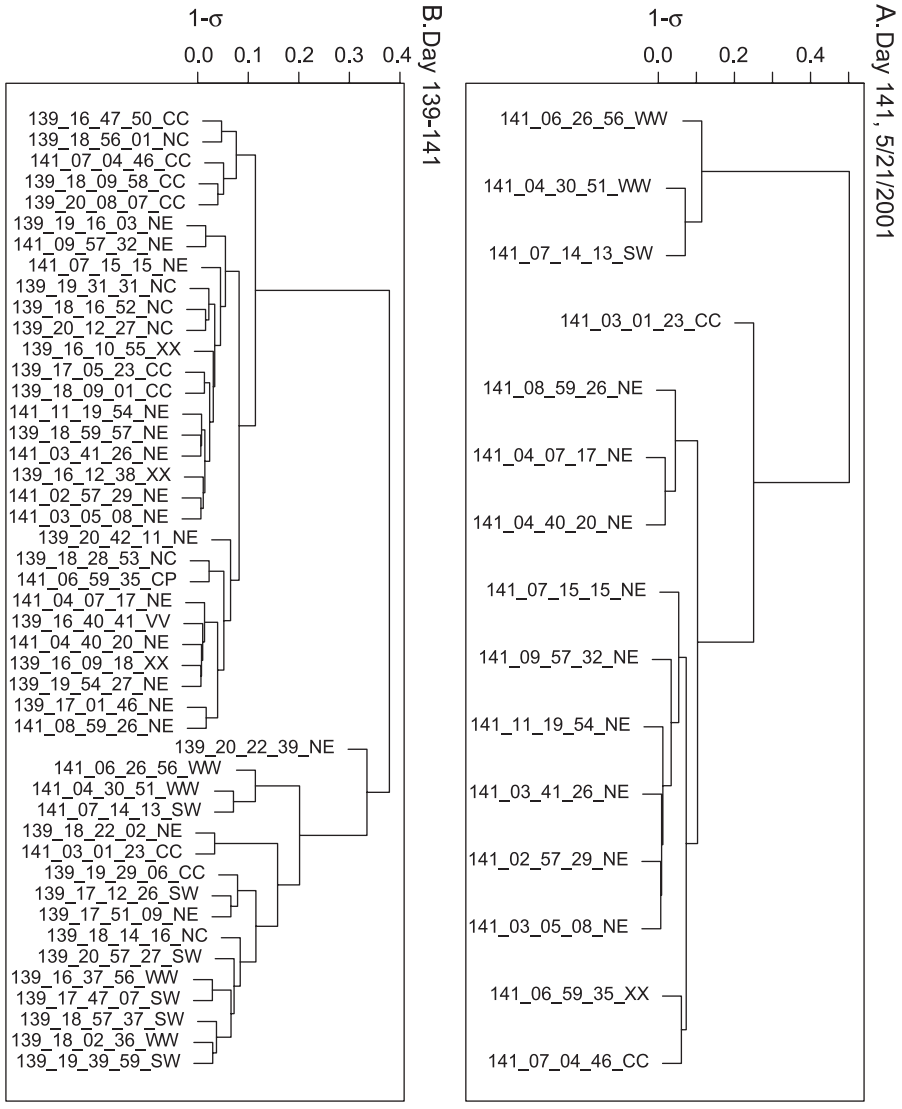

Fig. 5. Dendrograms of cluster analysis on (A) May 21 (Day 141) and (B) May 19 through May 20 (Days 139–140). Symbols and explanation are the same as in Fig. 4.

plumbing system, perhaps 200 m below the surface (Chouet et al., 2003). Hierarchical clustering was performed on the matrix of cross-correlation scores (σ), derived from the low-frequency signals alone. Results of the clustering are presented as dendrograms (Figs. 4 and 5), revealing clustering patterns of events, as well as the relative similarity among clusters.

Using differential acoustic travel times (FOR/HEL, Fig. 3) and seismic waveform shapes, each event was provided a tag (NE, SW, CC, NC) if it was clearly associated with a particular crater. Events that had indeterminate travel time, but exhibited a characteristic shape, were designated WW or VV, and those events that did not fall into any category were labeled XX. The flags were used on the dendrogram to verify that clusters are indeed vent or crater specific. The 14 events presented in Fig. 5A from May 21 illustrate distinct clusters of events, corresponding to the NEC, CC, and SWC. Events marked with NE are distinct

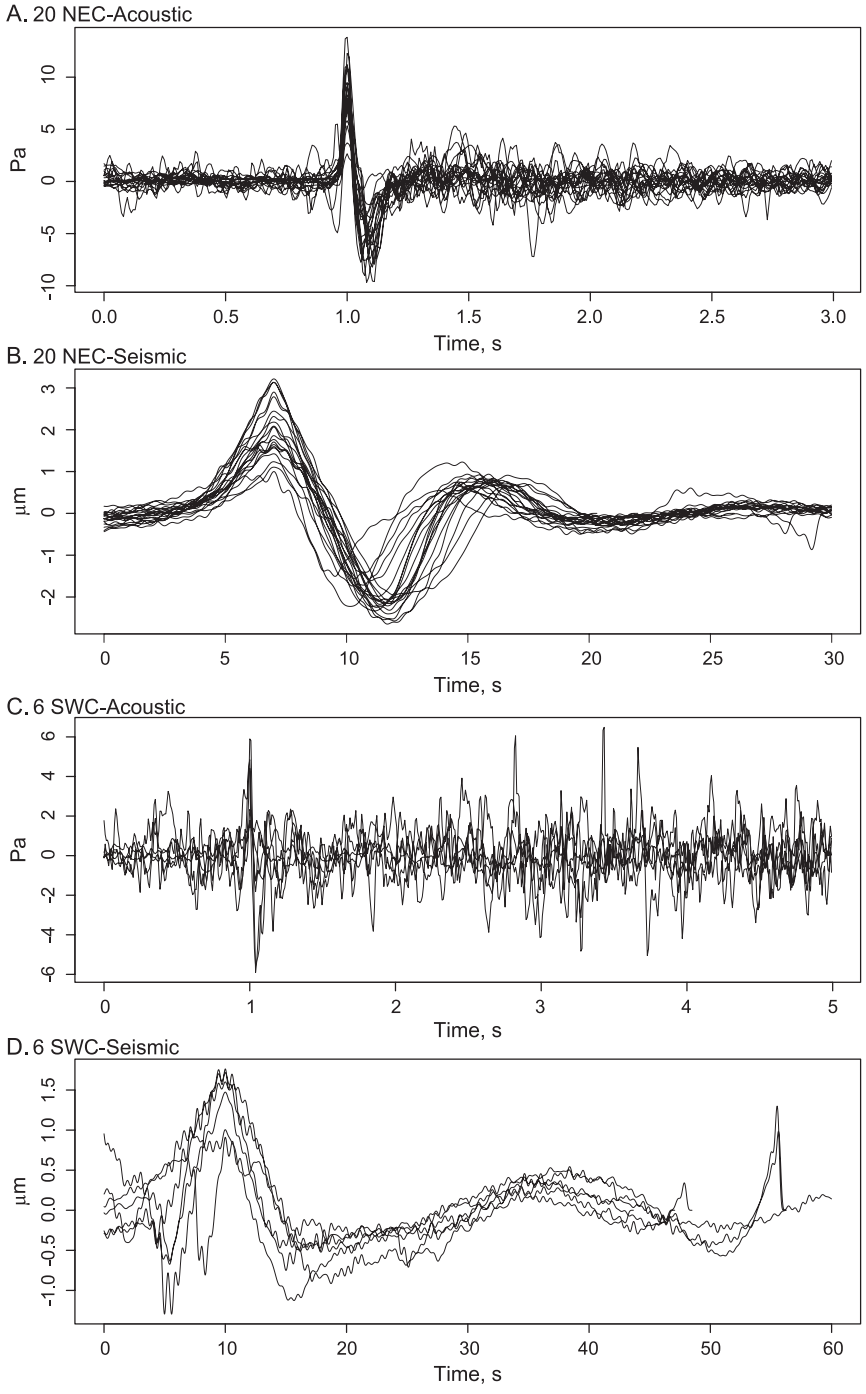

Fig. 6. Stacked acoustic and vertical seismic displacement records. All waveforms recorded on station FOR. The repetitive nature of the waveforms is revealed in stacked signals from (A–B) NEC (20 events), (C–D) SWC (six events), (E–F) Hornito vent (three events), (G) Puffer vent (four infrasound signals).

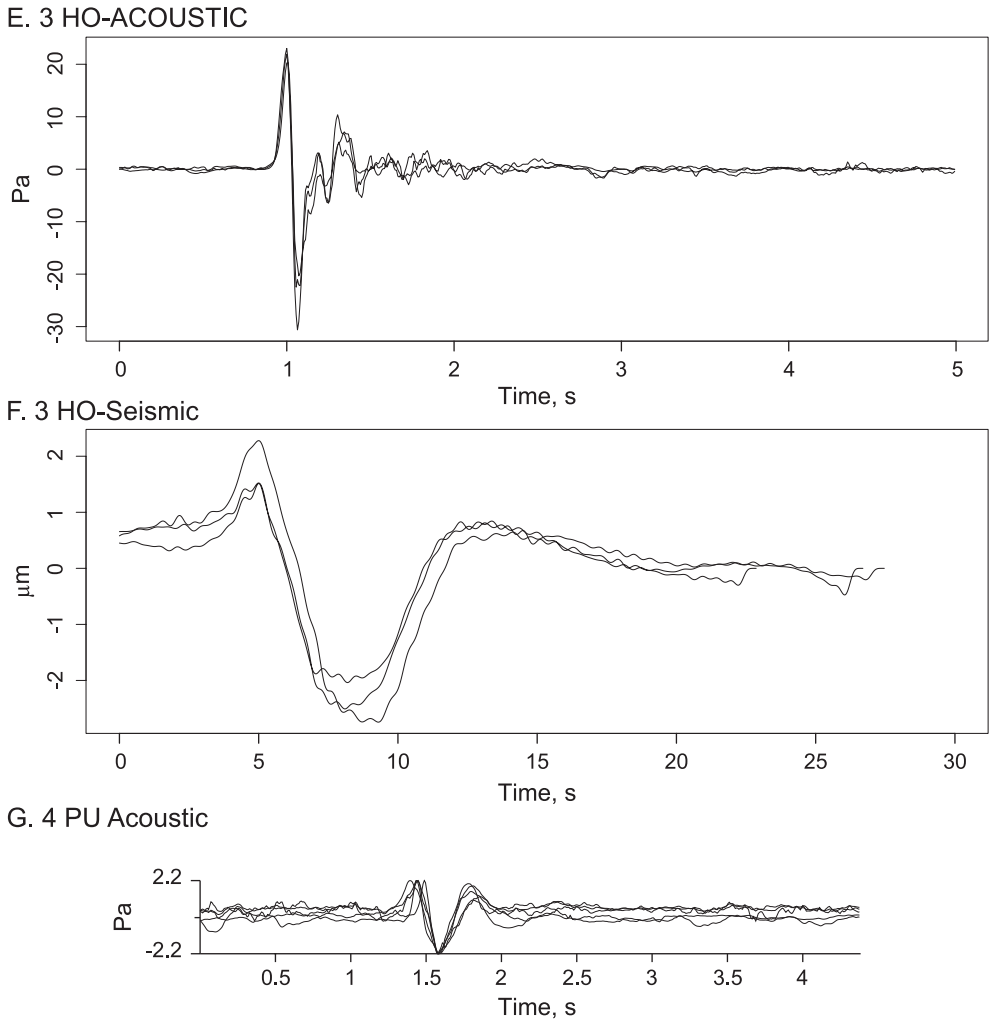

Fig. 6 (*continued*).

from SW and WW events. Events designated CC and XX branch away from the larger NE cluster, although there is some ambiguity regarding where the CC events fall relative to NE.

Separate clusterings for days 139 and 140 (Fig. 4) show a distinct partitioning of events from the NEC and the SWC, while it is evident that there are a few events that apparently do not follow the general rule. The presence of noise, or other subtle differences in the signals, causes a few events to be misplaced in clusters improperly diagnosed. Signals that could not be associated with craters based on travel-times, however, correctly cluster close to where they are expected to be, VV events in the NE cluster and WW events in the SW cluster. CC events group together and are more closely associated with the NE cluster than the SW cluster. Interestingly, XX events generally associate with the CC cluster or the NE cluster, but rarely with the SW cluster. Comparative shape of the waveforms can be observed in the structure of the dendrogram. The NEC produces the tightest dendrogram cluster, which is related to the fact that these explosions produce the simplest, and most repeatable displacement waveforms (Figs. 2B and 6A). The CC events, which appear to share a similar shape and period with the NEC events, share some

characteristics with the SWC events (Fig. 2A). We see that both events from the CC and NC display a slightly more complicated waveform morphology than signals produced by the majority of NEC events, yet have visually simpler waveforms than those with sources associated with SWC explosions. On the dendrograms, differences in waveform shape are reflected as longer stems linking individual waveforms. The repetitive character of waveform shapes and the simplicity or complexity of groups of associated waveforms can be further illustrated by plotting time series of seismic and acoustic signals from all three craters (Fig. 6). Note the relative consistency of NEC events (short stems, tight clustering) versus those designated from the SWC (longer stems).

7. Discussion

We have shown that we can distinguish characteristic signals among five of the eight active vents at Stromboli, during a season of elevated explosion activity in May 2001. Infrasonic acoustic waves, coupled with seismic signals, suggest that each of the vents has a unique signature, and can be distinguished, often visually from waveform character, but almost always from acoustic travel time differentials. The long-period signals used by Chouet et al. (2003) for moment tensor inversion were clearly apparent during our deployment in 2001, although in this paper, we have further identified slight variations consistently associated with one or another of the eight active vents located within tens of meters of each other. If the long-period signals are correctly modeled by dipping cracks deforming at depths greater than 200 m, we expect that variations in long-period signals that are consistently associated with specific vents indicate that more than two large faults were active in May 2001. In Chouet et al.'s (2003) analysis, the two different, long-period waveforms were produced by sources spatially separated by an estimated 40 m in depth. Cluster analysis presented here shows that NEC events differ considerably from SWC events, as noted by Chouet et al., but also include detailed long-period distinctions, as well as acoustic differences, that are attributed to specific vents located within the NEC (NC vent, for example). This is true to a lesser extent in the SWC, where the data are apparently less consistent. The cluster analysis for Day 140 illustrates the tight clustering of the NEC explosions versus the more dispersed (smaller correlation) SWC signals. Given the wavelengths of the signals used for cluster analysis, we exclude the possibility that these differences are related to path effects between source and receiver. We conclude that sources producing SWC explosions are in some way more heterogeneous than those associated with the NEC.

The Hornito vent, located in the central crater between the SWC and the NEC, apparently shares characteristics with both the NEC and the SWC events, although its distinctive acoustic signature provides a means to unequivocally associate it with a separate process, distinct from the main craters. The inference is that the subsurface plumbing system must include a geometry significantly more complex than the simple two crack model proposed by Chouet et al. (2003), especially for the more heterogeneous signals recorded from the SWC. Slugs rising from a common source at depth, perhaps 200–300 m below the summit must differentiate and flow through a labyrinth of shallow conduits, each providing its own particular source time signature. The data collected in this study (three broad band seismic stations) are unfortunately insufficient to provide a source inversion for precise geometry of the multiple cracks and conduits at Stromboli in 2001. Our results, however, indicate a more complex geometry than previously assumed for the plumbing of the conduit system.

8. Conclusions

In this study, quantitative and qualitative cluster analyses were used to separate characteristic signals in seismo-acoustic explosions at Stromboli in May, 2001. We demonstrate that very long-period signals are associated with events produced by all three of Stromboli's active craters. Comparison of the waveforms reveals that explosions from the Hornito and the NEC exhibit nearly identical impulsive acoustic signals, and differ significantly from explosions originating in SWC vents. The NEC events have been modeled as single bubble explosions, related to an individual slug rising through the conduit. Explosions from the SWC are shown to exhibit an emergent, high-

frequency infrasonic signal, which has been attributed to the bursting of many smaller bubbles (Ripepe et al., 1993) resulting in a complicated displacement seismogram. We show that cross-correlation cluster analysis of displacement waveforms produces crater-specific clusters, which are stable over a two-day period. Further analysis is needed to determine longer term stability of the clusters, in light of evidence from Ripepe et al. (1993), that the dynamical processes controlling eruption-related flux of matter from vents vary in time. Cluster dendrograms show that clusters of events from the NEC and the CC have greater similarity (in waveform shape) than those compared between the NEC and the SWC clusters or those compared across the SWC and CC clusters. The close relationship between the CC and HO vents and the NEC waveforms suggests that there is a connection in the plumbing system between these craters, although differences in the long-period signals indicate a more intricate conduit geometry than earlier expected.

Acknowledgements

The authors express their gratitude to Jeff Johnson, Jackie Caplan-Auerbach, Andy Harris and an anonymous reviewer for the extensive, thorough and helpful critical comments on this paper. Special thanks to Maurizio Ripepe for the guidance and support in the field during the data acquisition in May 2001.

References

Aster, R.C., Scott, J., 1993. Comprehensive characterization of waveform similarity in large microearthquake data sets. Bull. Seismol. Soc. Am. 83 (4), 1307–1314.

Beinat, A., Carniel, R., Iacop, F., 1994. Seismic station of Stromboli: 3. Component data acquisition system. Acta Vulcanol. 5, 221–222.

Benoit, J.P., McNutt, S.R., 1997. New constraints on source processes of volcanic tremor at Arenal Volcano, Costa Rica, using broadband seismic data. Geophys. Res. Lett. 24 (4), 449–452.

Blackburn, E.A., Wilson, L., Sparks, R.S.J., 1976. Mechanisms and dynamics of Strombolian activity. J. Geol. Soc. (Lond.) 132, 429–440.

Braun, T., Ripepe, M., 1993. Interaction of seismic and air waves recorded on Stromboli Volcano. Geophys. Res. Lett. 20 (1), 65–68.

Buckingham, M.J., Garces, M.A., 1996. Canonical model of volcano acoustics. J. Geophys. Res. 101 (4), 8129–8151.

Chouet, B., Hamisevicz, N., McGetchin, T.R., 1974. Photoballistics of volcanic jet activity at Stromboli, Italy. J. Geophys. Res. 79 (32), 4961–4976.

Chouet, B., Saccorotti, G., Dawson, P., Martini, M., Scarpa, R., De Luca, G., Milana, G., Cattaneo, M., 1999. Broadband measurements of the sources of explosions at Stromboli Volcano, Italy. Geophys. Res. Lett. 26 (13), 1937–1940.

Chouet, B., Dawson, P., Ohminato, T., Martini, M., Saccorotti, G., Giudicepietro, F., De Luca, G., Milana, G., Scarpa, R., 2003. Source mechanisms of explosions at Stromboli Volcano, Italy, determined from moment-tensor inversions of very-long-period data. J. Geophys. Res., 2019 (doi:10.1029/2002JB001919).

Del Pezzo, E., Guerra, I., Bascio, A.L., Luongo, G., Nappi, G., Scarpa, R., 1975. Microtremors and volcanic explosions at Stromboli—Part 2. Bull. Volcanol. 38 (4), 1023–1036.

Falsaperla, S., Schick, R., 1993. Geophysical studies on Stromboli Volcano—a review. Acta Vulcanol. 3, 153–162.

Falsaperla, S., Langer, H., Spampinato, S., 1998. Statistical analyses and characteristics of volcanic tremor on Stromboli Volcano (Italy). Bull. Volcanol. 60 (2), 75–88.

Frohlich, C., Davis, S.D., 1990. Single-link cluster analysis as a method to evaluate spatial and temporal properties of earthquake catalogues. Geophys. J. Int. 100 (1), 19–32.

Garces, M.A., 1997. On the volcanic waveguide. J. Geophys. Res. 102 (10), 22547–22564.

Garces, M.A., 2000. Theory of acoustic propagation in a multiphase stratified liquid flowing within an elastic-walled conduit of varying cross-sectional area. J. Volcanol. Geotherm. Res. 101 (1–2), 1–17.

Garces, M.A., McNutt, S.R., 1997. Theory of the airborne sound field generated in a resonant magma conduit. J. Volcanol. Geotherm. Res. 78 (3–4), 155–178.

Garces, M.A., Hagerty, M.T., Schwartz, S.Y., 1998. Magma acoustics and time-varying melt properties at Arenal Volcano, Costa Rica. Geophys. Res. Lett. 25 (13), 2293–2296.

Hartigan, J.A., 1975. Clustering Algorithms. John Wiley and Sons, New York. 350 pp.

Ihaka, R., Gentleman, R., 1996. R: a Language for Data Analysis and Graphics. Journal of Computational and Graphical Statistics 5 (3), 299–314.

Jaupart, C., Vergniolle, S., 1988. Laboratory models of Hawaiian and Strombolian eruptions. Nature 331, 58–60.

Jaupart, C., Vergniolle, S., 1989. The generation and collapse of a foam layer at the roof of a basaltic magma chamber. Journal of Fluid Mechanics 203, 347–380.

Johnson, J.B., Lees, J.M., 2000. Plugs and Chugs-Strombolian activity at Karymsky, Russia, and Sangay, Ecuador. J. Volcanol. Geotherm. Res. 101, 67–82.

Johnson, J.B., Lees, J.M., Gordeev, E., 1998. Degassing explosions at Karymsky Volcano, Kamchatka. Geophys. Res. Lett. 25 (21), 3999–4042.

Johnson, J.B., Aster, R.C., Ruiz, M.C., Malone, S.D., McChesney, P.J., Lees, J.M., Kyle, P.R., 2003. Interpretation and utility of infrasonic records from erupting volcanoes. J. Volcanol. Geotherm. Res. 121 (1–2), 15–63.

Kaufman, L., Rousseeuw, P.J., 1990. Finding Groups in Data. Wiley, New York, 342 pp.

Lees, J.M., 1997. Waveform and spatial clustering in high-frequency seismograms. In: Engl, H.W., Louis, A.K., Rundell, W. (Eds.), Inverse Problems in Geophysical Applications. Society for the Industrial Applications of Mathematics, Philadelphia, pp. 109–130.

Lees, J.M., 1998. Multiplet analysis at Coso Geothermal. Bull. Seismol. Soc. Am. 88 (5), 1127–1143.

Lo Bascio, A., Luongo, G., Nappi, G., 1973. Microtremors and volcanic explosions at Stromboli (Aeolian Islands). Bull. Volcanol. 37, 516–606.

Neuberg, J., Luckett, R., 1996. Seismo-volcanic sources on Stromboli Volcano. Ann. Geofis. 39 (2), 377–391.

Neuberg, J., Luckett, R., Ripepe, M., Braun, T., 1994. Highlights from a seismic broadband array on Stromboli Volcano. Geophys. Res. Lett. 21 (9), 749–752.

Ntepe, N., Dorel, J., 1990. Observations of seismic volcanic signals at Stromboli Volcano (Italy). J. Volcanol. Geotherm. Res. 43, 235–251.

Ripepe, M., 1996. Evidence for gas influence on volcanic seismic signals recorded at Stromboli. J. Volcanol. Geotherm. Res. 70 (3–4), 221–233.

Ripepe, M., Gordeev, E., 1999. Gas bubble dynamics model for shallow volcanic tremor at Stromboli. J. Geophys. Res. 104 (5), 10639–10654.

Ripepe, M., Rossi, M., Saccorotti, G., 1993. Image processing of explosive activity at Stromboli. J. Volcanol. Geotherm. Res. 54 (3–4), 335–351.

Ripepe, M., Poggi, P., Braun, T., Gordeev, E., 1996. Infrasonic waves and volcanic tremor at Stromboli. Geophys. Res. Lett. 23 (2), 181–184.

Ripepe, M., Coltelli, M., Privitera, E., Gresta, S., Moretti, M., Piccinini, D., 2001. Seismic and infrasonic evidences for an impulsive source of the shallow volcanic tremor at Mt. Etna, Italy. Geophys. Res. Lett. 28 (6), 1071–1074.

Schick, R., 1981. Source mechanism of volcanic earthquakes. Bull. Volcanol. 44, 491–497.

Vergniolle, S., Brandeis, G., 1994. Origin of the sound generated by Strombolian explosions. Geophys. Res. Lett. 21 (18), 1959–1962.

Vergniolle, S., Jaupart, C., 1990. Dynamics of degassing at Kilauea Volcano, Hawaii. J. Geophys. Res. 95 (B3), 2793–2809.

Vergniolle, S., Brandeis, G., Mareschal, J.C., 1996. Strombolian explosions: 2. Eruption dynamics determined from acoustic measurements. J. Geophys. Res. 101 (9), 20449–20466.

Washington, H.S., 1917. Persistance of vents at Stromboli and its bearing on volcanic mechanism. Geol. Soc. Am. Bull. 28, 248–278.

Wilson, L., Sparks, R.S.J., Walker, G.P.L., 1980. Explosive volcanic eruptions: IV. The control of magma properties and conduit geometry on eruption column behaviour. Geophys. J. R. Astron. Soc. 63 (1), 117–148.